Phosphatidylinositol 5-phosphate 4-kinase (PIP4K) regulates TOR signaling and cell growth during *Drosophila* development

Amit Gupta[a,1], Sarah Toscano[b,1], Deepti Trivedi[b,1], David R. Jones[c], Swarna Mathre[a], Jonathan H. Clarke[d], Nullin Divecha[c], and Padinjat Raghu[a,b,2]

[a]National Centre for Biological Sciences, Tata Institute of Fundamental Research, Gandhi Krishi Vignana Kendra Campus, Bangalore 560065, India; [b]Inositide Laboratory, Babraham Institute, Cambridge CB22 2AT, United Kingdom; [c]Patterson Institute for Cancer Research, University of Manchester, Manchester M20 4BX, United Kingdom; and [d]Department of Pharmacology, University of Cambridge, Cambridge CB2 1PD, United Kingdom

Edited by Pietro De Camilli, Yale University and Howard Hughes Medical Institute, New Haven, CT, and approved February 26, 2013 (received for review November 6, 2012)

During development, *Drosophila* larvae undergo a dramatic increase in body mass wherein nutritional and developmental cues are transduced into growth through the activity of complex signaling pathways. Class I phosphoinositide 3-kinases have an established role in this process. In this study we identify *Drosophila* phosphatidylinositol 5-phosphate 4-kinase (dPIP4K) as a phosphoinositide kinase that regulates growth during larval development. Loss-of-function mutants in dPIP4K show reduced body weight and prolonged larval development, whereas overexpression of dPIP4K results both in an increase in body weight and shortening of larval development. The growth defect associated with dPIP4K loss of function is accompanied by a reduction in the average cell size of larval endoreplicative tissues. Our findings reveal that these phenotypes are underpinned by changes in the signaling input into the target of rapamycin (TOR) signaling complex and changes in the activity of its direct downstream target p70 S6 kinase. Together, these results define dPIP4K activity as a regulator of cell growth and TOR signaling during larval development.

During postembryonic development, *Drosophila* larvae undergo a period of rapid growth that lasts for approximately 96 h during which larvae undergo rapid growth with body weight increasing by two log units. This dramatic increase in larval body weight is almost entirely underpinned by increases in the cell size of larval-specific endoreplicative tissues (1). The extent of growth during larval life is critical as adult body size in insects is predetermined during larval development. Consequently, larval growth is a carefully regulated process (2) and insect larvae must attain a so-called minimum viable weight to trigger developmental cues that signal termination of larval growth and the onset of pupal metamorphosis.

Several factors contribute to normal larval growth. At an organismal level, these include the availability of adequate nutrition, the ability to feed (reviewed in ref. 3), as well as endocrine signals that regulate nutrient utilization and coordinate growth with metamorphosis. At the cellular level, key contributors to larval growth are the activity of signaling cascades that transduce nutrient availability and regulate their utilization to generate cellular and body mass. These include the activity of *Drosophila* insulin-like peptides (DILPs) acting via the insulin receptor and that of the target of rapamycin (TOR) pathway. Phosphoinositide kinases have key roles within both the insulin (4) and TOR signaling pathways (5). The generation of phosphatidylinositol 3,4,5 trisphosphate (PIP_3) by class I phosphoinositide 3-kinases (PI3Ks) is an essential early step following insulin receptor activation. Likewise the generation of phosphatidylinositol 3-phosphate (PI3P) via class III PI3K/vacuolar protein sorting 34 (Vps34) is reported to be a key signaling input into TOR activity in mammalian cells (6).

Phosphoinositides are phosphorylated derivatives of phosphatidylinositol (PI), several of which are known to regulate fundamental cellular processes in eukaryotes. These phosphorylations are catalyzed by an evolutionarily conserved family of lipid kinases that are stereospecific with respect to the positions on the inositol headgroup that they can phosphorylate and also show specificity for their preferred substrate. One such enzyme is phosphatidylinositol 5-phosphate 4-kinase (PIP4K) previously known as type II phosphatidylinositolphosphate (PIP) kinase (7). In vitro, PIP4K enzymes can phosphorylate both PI5P and PI3P to produce $PI(4,5)P_2$ and $PI(3,4)P_2$, respectively (8, 9). Genes encoding PIP4K activity are present in sequenced metazoan genomes but not in those of unicellular eukaryotes such as yeast. PIP4K enzymes are biochemically distinct from the closely related family of phosphatidylinositol 4-phosphate 5 kinase (PIP5K). PIP5Ks use PI4P as a substrate to generate $PI(4,5)P_2$ and are presumed to underlie the synthesis of the major pools of cellular $PI(4,5)P_2$. PIP5Ks have been known to regulate many cellular processes including cell migration, focal adhesion assembly/disassembly, cell division, polarity, and vesicular trafficking (10). Functional analysis in vivo has shown that the distinct in vitro substrate specificity of PIP5K and PIP4K is also relevant to in vivo function (11–13), implying that PIP4Ks may modulate a set of cellular processes distinct from those controlled by PIP5Ks. However, in contrast to PIP5Ks little is known about the physiological functions of PIP4Ks.

Mammalian genomes contain three genes (α, β, and γ) that encode PIP4K activity. PIP4Kα encodes a protein localized primarily in the cytosol (reviewed in ref. 14); no in vivo function has been ascribed to this gene. PIP4Kβ encodes a protein that is nuclear localized (15) and its activity has been implicated in the regulation of cellular responses in the nucleus during UV irradiation (16). In addition, altered PIP4Kβ activity has been reported to regulate the sensitivity of mammalian cells to insulin signaling. Expression of PIP4Kβ in CHO cells results in down-regulation of PIP_3 production and AKT (protein kinase B) phosphorylation in response to insulin stimulation (17), whereas skeletal muscle cells from PIP4Kβ$^{-/-}$ mice show enhanced sensitivity to insulin stimulation (18). PIP4Kγ encodes a protein that appears to localize to endomembrane compartments whose identity is unclear (19). Whereas these studies suggest important cellular functions for PIP4K enzymes, the physiological significance and the mechanism by which this unique

Author contributions: P.R. designed research; A.G., S.T., D.T., D.R.J., S.M., J.H.C., and N.D. performed research; D.T. contributed new reagents/analytic tools; A.G., S.T., D.R.J., S.M., J.H.C., N.D., and P.R. analyzed data; and A.G. and P.R. wrote the paper.

The authors declare no conflict of interest.

This article is a PNAS Direct Submission.

[1]A.G., S.T., and D.T. contributed equally to this work.

[2]To whom correspondence should be addressed. E-mail: praghu@ncbs.res.in.

This article contains supporting information online at www.pnas.org/lookup/suppl/doi:10.1073/pnas.1219333110/-/DCSupplemental.

class of lipid kinase exerts its effects remain unclear. In this study, we have analyzed the single PIP4K gene encoded in the *Drosophila* genome. Our studies reveal a functional role for *Drosophila* PIP4K (dPIP4K) activity in regulating cell growth via the TOR pathway during *Drosophila* larval development.

Results

Single Gene Encoding PIP4K in *Drosophila*. We used mouse PIP4KIIα sequence as a query and performed a BLAST analysis of the completed genome sequence of *Drosophila*. This revealed a single hit corresponding to the gene named CG17471. CG17471 is located on chromosome 4, cytogenetic position 102F8. Computationally, two splice variants of CG17471 are predicted that differ in a noncoding exon but encode an identical 404-amino-acid protein. Analysis of the encoded protein sequence with INTERPRO revealed that amino acids 31–403 encode a "PIP kinase catalytic domain" [Interpro (IPR) 002498]. Inspection of the region corresponding to the "activation loop" (20) whose sequence is reported to correlate with PIP5K versus PIP4K activity (13) suggests that CG17471 encodes a PIP4K activity (Fig. 1*A*). Finally inspection of the single amino acid at position 381 within the activation loop of human PIP4K (Fig. 1*A*, arrow), which is reported to define the stereospecific activity of a PIPK enzyme (12), revealed that the equivalent residue in CG17471 is an alanine rather than a glutamate. Together these bioinformatic analyses suggest that CG17471 encodes the single PIP4K (hereafter called dPIP4K) in the *Drosophila* genome. Analysis of genome sequences of the 11 other *Drosophila* species as well as that of other sequenced insect genomes reveals the existence of a single PIP4K-like gene.

We identified a full-length cDNA for the *dPIP4K* locus (LD10864). This cDNA includes a 404-amino-acid ORF that encodes a protein identical to that predicted by computational analysis of the *dPIP4K* locus (Fig. 1*B*). We expressed this cDNA and tested the activity of purified recombinant protein in an in vitro lipid kinase assay. When presented with PI5P as a substrate, this protein showed PIP4K activity (Fig. 1*C*), being able to convert PI5P into PI(4,5)P_2 but showed no activity toward PI or PI3P substrates (Fig. S1). dPIP4K also showed minimal activity toward PI4P as a substrate (Fig. S1) and this substrate specificity recapitulates that of human PIP4Kα under the same conditions (8, 21). Taken together these data show that *dPIP4K* encodes a functional PIP4K activity.

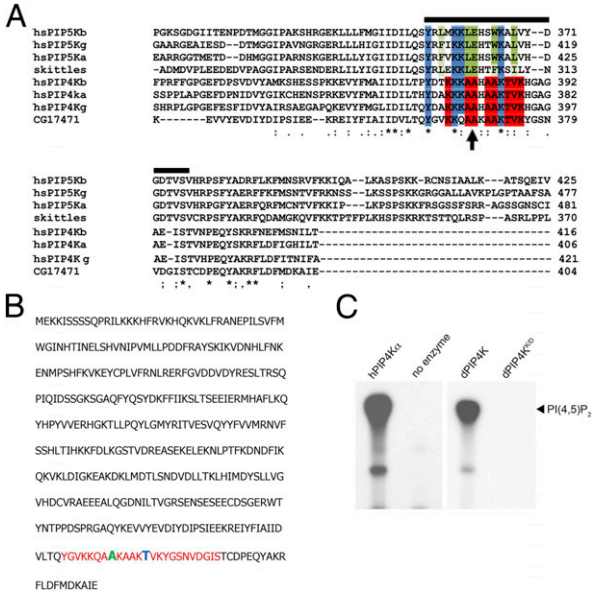

Fig. 1. (*A*) Multiple alignment of a set of sequences for PIP4K and PIP5K genes. Alignment for the C-terminal end of the proteins that includes part of the PIPK domain is shown. hs, *Homo sapiens*; a, alpha; b, beta; g, gamma; Skittles, a *Drosophila* PIP5K; CG17471, a *Drosophila* PIP4K. The region corresponding to the activation loop is marked by a solid black line. In the region of the activation loop, residues that are identical in both PIP4K and PIP5K are marked in dark blue with conserved substitutions in light blue. Residues conserved among PIP5K proteins are marked in green with conserved substitutions in light green. Residues conserved among PIP4K proteins are marked in red. Arrow indicates the single residue that has been shown to determine PIP5K vs. PIP4K activity. (*B*) Protein sequence encoded by the ORF of the cDNA clone LD10864 that encodes dPIP4K. The sequence of the activation loop is marked in red. The single residue with the activation loop that has been shown to determine PIP4K vs. PIP5K for the human protein is shown in green. The residue shown to be phosphorylated by protein kinase D (PKD) in hsPIP4Kb is shown in blue. (*C*) Lipid kinase activity of wild-type and mutant dPIP4K. Recombinant phosphatidylinositol (PtdIns) 5-phosphate 4-kinase protein expressed and purified from constructs encoding the human PIP4Kα isoform (hPIP4K), wild-type *D. melanogaster* PIP4K (dPIP4K), and a kinase-dead (D271K) mutant of the *Drosophila* enzyme (dPIP4K$^{K/D}$) were assayed for lipid kinase activity as described in *SI Materials and Methods*. Radiolabeled PI(4,5)P_2 product (arrowhead) was identified by silica TLC and autoradiography. Samples from different sections of the same TLC plate are aligned for convenience.

***dPIP4K* Regulates PI5P Levels in Vivo.** A loss-of-function mutant in this gene was generated using ends-out homologous recombination. The resulting mutant allele (*dPIP4K^{29}*) disrupts the kinase domain and should produce no functional protein (Fig. 2*A*). Using an antibody generated against dPIP4K, we found that *dPIP4K^{29}* is a protein null allele (Fig. 2*B*).

To understand the biochemical consequences of dPIP4K loss of function we measured the levels of PI4P, PI5P, and PI(4,5)P_2 in lipid extracts from flies. This revealed that PI5P levels in *dPIP4K^{29}* were twice that measured in wild-type controls (Fig. 2*D*); by contrast, the levels of PI4P (Fig. 2*C*) and PI(4,5)P_2 levels were not reduced (Fig. 2*F*). We reconstituted *dPIP4K^{29}* with either a wild-type dPIP4K transgene or the point mutant allele [amino acid 271 (D271K) was mutated from aspartic acid to lysine, Fig. 1*C*] that is kinase dead. Transgenes were expressed using the ubiquitous actin-GAL4 driver that drives expression throughout the fly. Biochemical analysis revealed that when *dPIP4K^{29}* is reconstituted with a wild-type transgene, the elevated PI5P levels were reversed toward wild-type levels (Fig. 2*E*); this was not seen with a kinase dead transgene (Fig. 2*E*). These results strongly suggest that the kinase activity of dPIP4K is required to maintain PI5P levels in vivo.

dPIP4K Activity Regulates Growth and the Rate of Larval Development. Although *dPIP4K^{29}* embryos develop into homozygous adults with apparently normal external morphology, a detailed analysis of larval growth revealed significant developmental defects. Whereas both wild-type and *dPIP4K^{29}* animals showed equivalent body weight soon after hatching, *dPIP4K^{29}* larvae weighed less than their wild-type counterparts at multiple time points during development (Fig. 3*A*). The maximum difference in body weight was at 60 h posthatching (at 22 °C) when *dPIP4K^{29}* larvae weighed approximately 54% of controls; toward the end of larval development this difference is relatively reduced (*dPIP4K^{29}* larvae weigh approximately 85% of wild-type controls) but with a delay of approximately 12 h (Fig. 3*A*). The reduction in body weight was substantially rescued by reconstitution of *dPIP4K^{29}* using a wild-type dPIP4K transgene (Fig. 3 *B* and *C*). Consistent with the idea that adult body size in insects is predetermined during larval development we observed that newly eclosed adult *dPIP4K^{29}* flies weighed less than the wild-type controls (Fig. 3*H*). Moreover, we observed that ubiquitous overexpression of dPIP4K in larval cells increased body weight compared with controls (Fig. 3 *D* and *E*). Collectively these data strongly suggest that dPIP4K function is required to regulate growth during larval development.

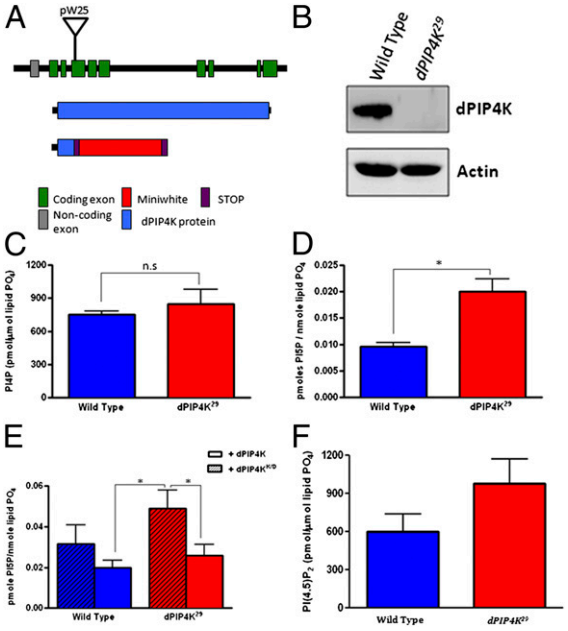

Fig. 2. Generation of a loss-of-function allele of dPIP4K. (*A*) Representation of the genomic region encoding dPIP4K. Exons are shown as rectangles including noncoding (gray) and coding (green) exons. The site of insertion of the recombineering construct is marked (pW25). The protein coded by dPIP4K is marked along with the mutant allele generated after recombination (*dPIP4K*^{29}). The miniwhite marker of the targeting construct is shown (red rectangle) as well as the stop codons in all three frames on both strands (purple). (*B*) Western blot from fly head extracts showing the absence of dPIP4K protein in *dPIP4K*^{29}. Actin has been used as a loading control. (*C*–*F*) Phosphoinositide levels in extracts from *dPIP4K*^{29}. Mass assays of whole body lipid extracts from flies aged 0–24 h. *Y*-axis shows the average ± SEM of three independent estimations. In all cases, PI4P or PI5P or PI(4,5)P_2 levels are expressed per unit of organic phosphate in the extracts. (*C*) PI4P levels in wild type and *dPIP4K*^{29}. (*D*) PI5P levels from the same extracts. (*E*) Reversion of PI5P levels in *dPIP4K*^{29} lipid extracts toward wild-type levels by a wild-type dPIP4K transgene (+dPIP4K, open bars) but not by a kinase dead version of the enzyme (+dPIP4K$^{K/D}$, hatched bars). (*F*) PI(4,5)P_2 levels in wild-type and *dPIP4K*^{29} extracts.

Following embryogenesis, the time taken to complete larval development is inversely related to gain in body weight (2). Consistent with this idea, we found that the time spent in larval development before pupariation was longer in *dPIP4K*^{29} compared with controls. Whereas approximately 80% of wild-type larvae had pupariated by 5 d posthatching, only 20% of *dPIP4K*^{29} animals had done so (Fig. 3*F*). *dPIP4K*^{29} animals continued larval development several days after wild-type controls had all pupariated. Conversely, larval development was accelerated by overexpressing dPIP4K (Fig. 3*I*), whereas larvae overexpressing a kinase dead transgene pupariated with a delay (Fig. 3*I*). We also reduced dPIP4K transcripts in wild-type larvae by expressing a transgenic RNAi construct ubiquitously during larval development; this resulted in a reduction in body weight as well as delayed pupariation reminiscent of that seen in *dPIP4K*^{29} (Fig. S2). Together these findings imply that the level of dPIP4K activity regulates body weight and developmental rate during larval development.

dPIP4K Regulates Cell Size and phosphorylated p70 S6 kinase (pS6K) in Larval Cells. Because most growth in *Drosophila* larvae is through an increase in the cell size of endoreplicative tissues, we asked if cell size was altered in *dPIP4K*^{29}. Analysis of salivary glands revealed that the average size of cells was lower in *dPIP4K*^{29} compared with wild type (Fig. 4 *A* and *B*). Notably, the reduced cell size in *dPIP4K*^{29} was rescued by reconstitution with a dPIP4K transgene (Fig. 4 *A* and *B*) and dPIP4K overexpression in larval cells resulted in an increase of salivary gland cell size (Fig. 4*I*). These results highlight the requirement of dPIP4K function in regulating cell size in larval endoreplictaive tissues.

In both *Drosophila* and mammals, the protein kinase AGC family member, p70 S6 kinase (S6K) is a positive regulator of cell size (22) and its activity is regulated by phosphorylation. We found that in larval extracts from *dPIP4K*^{29}, the levels of phosphorylated S6K (pS6K) were lower than in controls (Fig. 4*C*). Conversely, overexpression of wild-type dPIP4K ubiquitously in larvae (Fig. 4*D*) but not a kinase dead version (Fig. 4*E*) resulted in increased pS6K levels. To test the role of reduced pS6K levels in the growth defects of *dPIP4K*^{29}, we overexpressed *Drosophila* S6K (dS6K) in larval cells. The ubiquitous overexpression of dS6K in wild-type larvae results in an increase in larval body weight to about 1.25 times that of controls (Fig. 4 *F* and *G*). In

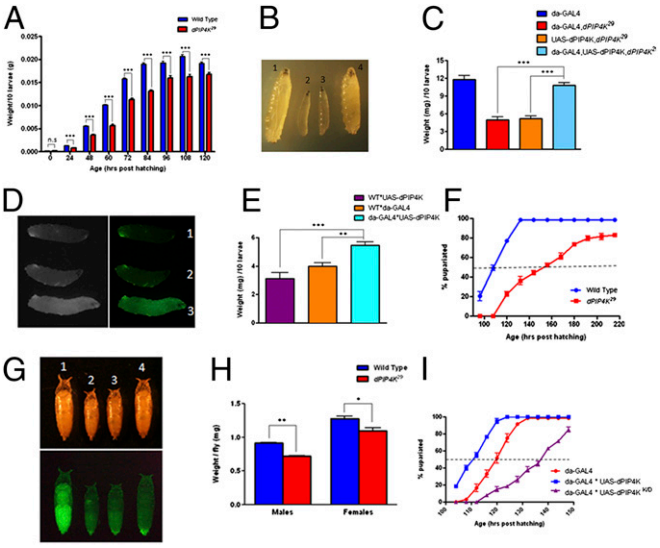

Fig. 3. Abnormal larval development in *dPIP4K*^{29}. (*A*) Developmental profile of larvae showing slower rate of weight gain in *dPIP4K*^{29} compared with wild-type controls under the same conditions. Experiments were done at 22 °C. *Y*-axis shows the average weight of 10 larvae ± SEM ($n = 100$). *X*-axis shows the age of larvae in hours posthatching. (*B*) Micrographs of individual larvae at 72 h posthatching of the following genotypes: (*1*) da-Gal4;UAS-dPIP4K; *dPIP4K*^{29}, (*2*) da-Gal4;*dPIP4K*^{29}, (*3*) UAS-dPIP4K;*dPIP4K*^{29}, and (*4*) da-Gal4. (*C*) Rescue of the larval weight deficit of *dPIP4K*^{29} by a wild-type dPIP4K::GFP transgene expressed using da-GAL4. *Y*-axis shows the average weight per 10 larvae ± SEM ($n = 70$). Weight measurements were done at 72 h posthatching at 23 °C. (*D*) Micrographs showing the effect of overexpression of dPIP4K::GFP on larval size. (*Left*) Bright field images. (*Right*) GFP images. Genotypes are: (*1*) da-GAL4, (*2*) UAS-dPIP4K::GFP, and (*3*) da-GAL4*UAS-dPIP4K::GFP. (*E*) Average weight of larvae overexpressing dPIP4K. *Y*-axis shows the average weight per 10 larvae ± SEM ($n = 50$). Weight measurements were done at 60 h posthatching at 23 °C. (*F*) Comparison of pupariation rates seen in *dPIP4K*^{29} and wild-type controls. *X*-axis shows time in hours posthatching. *Y*-axis shows the cumulative percentage of larvae (average of three independent experiments) that have pupariated at any given time point. The dotted line indicates the level of 50% pupariation. (*G*) Micrographs of individual pupae of the following genotypes: (*1*) da-Gal4;UAS-dPIP4K;*dPIP4K*^{29}, (*2*) da-Gal4;*dPIP4K*^{29}, (*3*) UAS-dPIP4K;*dPIP4K*^{29}, and (*4*) da-Gal4. (*Upper*) Bright field images. (*Lower*) GFP images. (*H*) Average weight of newly eclosed (0–24 h old) wild-type and *dPIP4K*^{29} adult flies. *Y*-axis shows the average weight per fly ± SEM ($n = 50$). (*I*) Comparison of pupariation rates seen in animals overexpressing wild-type and K/D dPIP4K ubiquitously. *X*-axis shows time in hours posthatching. *Y*-axis shows the cumulative percentage of larvae (average of three independent experiments) that have pupariated at any given time point. The dotted line indicates the level of 50% pupariation. The hastening and delay in 50% pupariation of larvae overexpressing wild-type and K/D dPIP4K, respectively, was statistically significant compared with nonexpressing control (*P value* <0.001 vs. da-GAL4).

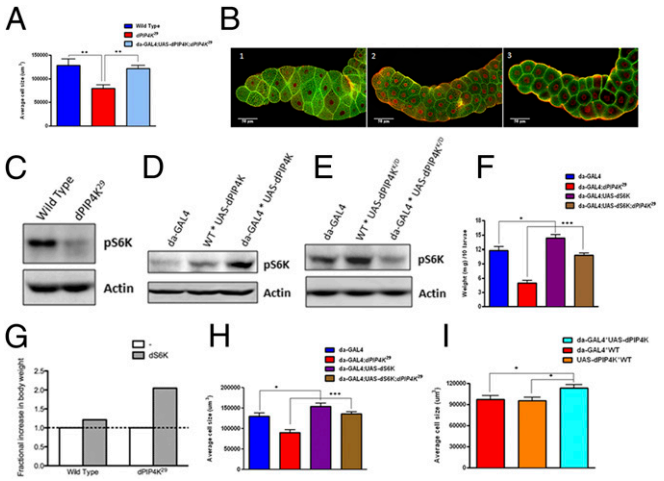

Fig. 4. Changes in salivary gland cell size in relation to dPIP4K activity. (*A*) Average size of salivary gland cells from wild-type, *dPIP4K*^{29}, and *dPIP4K*^{29} larvae reconstituted with a wild-type dPIP4K transgene expressed using da-GAL4. Measurements were done on wandering third instar larvae grown at 23 °C. *Y*-axis shows the average size of cells in the salivary gland ± SEM ($n = 5$). (*B*) Individual images of the secretory part of the salivary gland from larvae of following genotypes: (*1*) wild type, (*2*) *dPIP4K*^{29}, and (*3*) da-Gal4;UAS-dPIP4K; *dPIP4K*^{29}. Nucleus is stained orange and the membranes are stained green. Western blot analysis for the levels of pS6K: (*C*) In wild-type and *dPIP4K*^{29} larval extracts. (*D*) In animals overexpressing dPIP4K using da-GAL4. (*E*) In animals overexpressing a K/D version of dPIP4K. All extracts were prepared from wandering third instar larvae and levels of actin were used as a loading control. (*F*) Average weight of larvae in which dS6K was overexpressed. *Y*-axis shows the average weight per 10 larvae ± SEM ($n = 80$). Weight measurements were done at 72 h posthatching at 23 °C. (*G*) Fractional increase in body weight of larvae overexpressing dS6K. *Y*-axis represents the ratio of the average weight of larvae overexpressing dS6K in relation to non-overexpressing controls. Thus, (–) indicates wild-type or *dPIP4K*^{29} animals not overexpressing dS6K and (dS6K) indicates animals overexpressing a dS6K transgene. (*H*) Average size of salivary gland cells from larvae in which dS6K was overexpressed and (*I*) in larvae overexpressing dPIP4K. Measurements were done on wandering third instar larvae grown at 23 °C. *Y*-axis shows the average size of cells in the salivary gland ± SEM ($n = 5$ for both *H* and *I*). WT, wild type.

dPIP4K^{29} animals a similar overexpression of dS6K resulted in an approximately 2.25 times increase in bodyweight (Fig. 4*G*) such that the body weight was restored almost back to wild-type levels (Fig. 4*F*). Further, analysis of salivary gland cell size showed that in these animals salivary gland cell size was also reverted back toward wild type (Fig. 4*H*). These observations imply that reduced S6K activity underpins the reduced cell size and body weight observed in *dPIP4K*^{29} larvae.

Reduced TOR Activity in *dPIP4K*^{29} Larvae. The phosphorylation of S6K is principally mediated by the Ser/Thr kinase TOR, specifically the TOR complex 1 (TORC1) (23). To test the levels of functional TORC1, we grew larvae on food containing 2 μM rapamycin, a small molecule that universally inhibits the TORC1 complex (24) (but which may also inhibit TOR complex 2 (TORC2) in some settings) and measured the rate of larval development. As previously reported (25), we found that wild-type larvae grown on food containing rapamycin show a delay in larval development. Whereas approximately 80% of wild-type animals growing on control food had pupariated by day 5 post-hatching, none of the animals grown on 2 μM rapamycin had pupariated by this time point (Fig. 5*A*). The response of *dPIP4K*^{29} larvae to rapamycin treatment was dramatically different. Whereas 50% of *dPIP4K*^{29} larvae grown on control medium had pupariated by day 7, there were no pupae seen among *dPIP4K*^{29} larvae grown on 2 μM rapamycin. Even at 14 d posthatching <50% of *dPIP4K*^{29} animals grown on rapamycin had pupated, whereas >80% of animals grown on control food had done so (Fig. 5*A*). These results highlight the enhanced sensitivity of *dPIP4K*^{29} to rapamycin and suggest that TORC1 activity in reduced in *dPIP4K*^{29} larvae compared with wild type. Conversely, when grown on rapamycin-containing food, animals overexpressing dPIP4K were less sensitive to rapamycin and showed accelerated development compared with nonoverexpressing controls (Fig. 5*B*).

We also studied the phosphorylation of protein kinase B (AKT) at S505 (p-AKT^{S505}, equivalent to S473 in mammalian AKT) by the rapamycin-insensitive TORC2 complex (26). AKT is a key regulator of cellular growth in response to nutrient and growth factor signaling. These studies revealed that the level of p-AKT^{S505} was substantially reduced in protein extracts from wandering third instar larvae of *dPIP4K*^{29} compared with controls (Fig. 5*C*), implying that the activity of TORC2 is also down-regulated in cells lacking dPIP4K activity. Conversely, overexpression of dPIP4K during larval development results in an increase in the levels of p-AKT^{S505} (Fig. 5*D*), whereas overexpression of a kinase dead

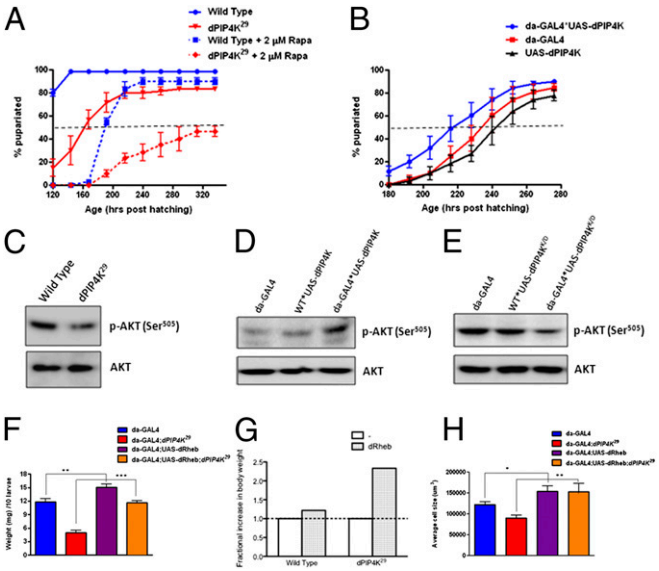

Fig. 5. Altered TOR signaling in *dPIP4K*^{29} larvae. (*A*) Rate of pupariation of wild-type and *dPIP4K*^{29} larvae grown posthatching on fly food containing 2 μM rapamycin or an equal volume of vehicle control ($n = 80$). (*B*) Rate of pupariation of larvae overexpressing dPIP4K and nonexpressing controls grown on food containing 2 μM rapamycin. In both cases, *y*-axis shows the cumulative percentage of larvae (average of three independent experiments) pupariated at a given time posthatching. *X*-axis shows the time in hours posthatching. The dotted line indicates the level of 50% pupariation. The hastening in 50% pupariation of larvae overexpressing dPIP4K was statistically significant compared with nonexpressing controls (*P value* <0.05 vs. da-GAL4 and *P value* <0.01 vs. UAS-dPIP4K). Western blots from protein extracts of third instar larvae that have just initiated wandering behavior. (*C*) Reduced phosphorylation of AKT using an antibody that detects phosphorylation at Ser505 [p-AKT(Ser^{505})]. (*D*) pAKT levels in larvae overexpressing wild-type dPIP4K ubiquitously, and (*E*) K/D dPIP4K. Total AKT levels have been used as a loading control. (*F*) Average weight of larvae in which dRheb was overexpressed. *Y*-axis shows the average weight per larva ± SEM ($n = 80$). Weight measurements were done at 72 h posthatching at 23 °C. (*G*) Fractional increase in body weight of larvae overexpressing dRheb. *Y*-axis represents the ratio of the average weight of larvae overexpressing dS6K in relation to nonoverexpressing controls. Thus, (–) indicates wild-type or *dPIP4K*^{29} animals not overexpressing dRheb and (dRheb) indicates animals overexpressing a dRheb transgene. (*H*) Average size of salivary gland cells from larvae in which dRheb was overexpressed. Measurements were done on wandering third instar larvae grown at 23 °C. *Y*-axis shows the average size of cells in the salivary gland ± SEM ($n = 5$). WT, wild type.

(K/D) version of dPIP4K resulted in reduced p-AKT^{S505} levels (Fig. 5*E*).

Overexpression of Ras Homolog Enriched in Brain (Rheb) Rescues the Growth Defect of *dPIP4K^{29}*. A key signaling input that regulates TOR activity is the small GTPase Ras homolog enriched in brain (Rheb) (27). To test if signaling inputs that regulate TOR activity were altered, we studied the effect of overexpressing *Drosophila* Rheb (dRheb). Overexpression of dRheb in wild-type larvae results in a small but consistent increase in body weight (Fig. 5*F*). When dRheb was overexpressed in *dPIP4K^{29}* larvae, there was a dramatic increase in body weight such that these larvae now weighed almost as much as wild type (Fig. 5*F*). The proportional increase in body weight was nearly 2.25 times compared with *dPIP4K^{29}* larvae not overexpressing dRheb (Fig. 5*G*). Analysis of salivary gland cell size in *dPIP4K^{29}* larvae overexpressing dRheb showed that the reduced cell size in *dPIP4K^{29}* was reverted back toward wild type (Fig. 5*H*). These findings strongly suggest that the underlying reason for the reduced growth and TORC activity in *dPIP4K^{29}* is a lack of signaling input to stimulate TOR activity via Rheb.

Discussion

During *Drosophila* larval development, nutritional and environmental cues are transduced into cellular growth and increased body size. In this setting generation of the phosphoinositides, PIP_3 and PI3P, play an important role and the kinases that synthesize these lipids namely class I and class III PI3K, respectively, are established regulators of cellular growth. In this study, we report the identification of dPIP4K as a lipid kinase that regulates growth during *Drosophila* development. We find that a null mutant in dPIP4K shows impaired growth during larval development. This phenotype is reminiscent of that seen in a mouse knockout of PIP4Kβ (18); these mice are reported to be smaller than wild-type controls and together with our findings suggest an evolutionarily conserved role for PIP4K in regulating growth in metazoans. We also found that overexpression of dPIP4K results in increased larval body weight. Thus, not only is dPIP4K required for normal larval development; the activity of this enzyme is also able to regulate weight gain and developmental rate in *Drosophila*.

The larval growth defect in *dPIP4K^{29}* was not due to an inability to feed (Fig. S3*A*) and transcripts for the major DILPs (DILP2 and DILP5) that are known to regulate larval growth in response to nutrients (28) were not altered (Fig. S3*B*), suggesting that defective DILP production is unlikely to underlie the growth defects of *dPIP4K^{29}*. In this study, we found that dPIP4K is a regulator of cell size. The cell size reduction in *dPIP4K^{29}* was accompanied by lowered levels of pS6K and could be rescued by overexpression of dS6K (Fig. 4). S6K has a well-established and evolutionarily conserved role in determining cell size (22). Our findings define dPIP4K acting via S6K as an important regulator of cell size during metazoan development.

In addition to reduced levels of pS6K, a signaling output of TORC1, *dPIP4K^{29}* larvae showed enhanced sensitivity to growth on rapamycin (Fig. 5*A*), supporting the conclusion that TORC1 activity is down-regulated in *dPIP4K^{29}* larvae. We also found that phosphorylation of AKT at Ser505, a signaling output of the TORC2 complex, was substantially reduced in *dPIP4K^{29}*. Thus, lack of dPIP4K results in a reduction in the signaling output of both TORC1 and TORC2 complexes in larvae. An economical interpretation of these observations is that the function of conserved components of both complexes might be down-regulated in *dPIP4K^{29}* larvae. These could include (*i*) changes in the conserved protein components or the subcellular localization of both TOR complexes. (*ii*) An alternative possibility is that signaling inputs needed to activate the TORC complexes are impaired in the absence of dPIP4K. Our observation that overexpression of Rheb, a known direct activator of the TORC1 complex, can rescue the growth defect in *dPIP4K^{29}* has two implications. First, it suggests that the intrinsic activity of the TORC1 complex in *dPIP4K^{29}* cells is normal to the extent that it can be stimulated by Rheb. Second, that the underlying reason for the reduced growth in *dPIP4K^{29}* cells is most likely a lack of signaling input to stimulate TORC1 activity. Our observation of increase in larval body mass, cell size, rate of larval development, and enhanced TOR-dependent phosphorylation of AKT and S6K seen with dPIP4K overexpression (in a kinase-dependent manner) further emphasize the fact that dPIP4K activity can regulate the activity of both TORC1 and TORC2. This observation provides compelling evidence of a role for the kinase activity of dPIP4K in regulating TOR signaling at or above the level of Rheb in *Drosophila* larval cells. In summary, our findings suggest that dPIP4K could be an additional regulator of nutritional or metabolic cues critical for regulating cell growth during *Drosophila* larval development via TORC activity.

Since the description of its distinctive enzymatic activity in vitro (8, 9), the biochemical activity relevant to the function of PIP4K enzymes in vivo has been unclear. In this study, we found that flies lacking the only PIP4K gene in the *Drosophila* genome show increased levels of PI5P. This elevation of PI5P levels was dependent on the kinase activity of dPIP4K (Fig. 2*E*), implying that the kinase activity of dPIP4K regulates PI5P levels in vivo. Although in vitro dPIP4K shows minimal activity to PI4P as a substrate, we found no changes in the levels of PI4P, suggesting that PIP4K activity is unlikely to be involved in the regulation of PI4P levels in vivo. Finally, the observation that $PI(4,5)P_2$ levels were not reduced in *dPIP4K^{29}* suggests that this enzyme is not required to maintain global levels of $PI(4,5)P_2$. Collectively our biochemical analysis of *dPIP4K^{29}* strongly suggests that in vivo, the lipid kinase activity of dPIP4K is required to regulate PI5P levels (Fig. 2 *D* and *E*). Biochemical fractionation (Fig. S4) suggest that endogenous dPIP4K is present both at the plasma membrane and also to some extent at some internal endomembranes. Thus, the elevated levels of PI5P seen in *dPIP4K^{29}* may occur at either of these subcellular locations. This is consistent with the previously reported enrichment of PI5P at the plasma membrane but also in intracellular membrane such as the Golgi (29).

Although no in vivo targets of PI5P have been clearly demonstrated, a number of proteins that carry a plant homeodomain domain have been reported to bind PI5P in vivo (30). In addition, in mammalian systems, it has been proposed that PI5P may regulate key molecules in the signaling pathway that mediates insulin signaling, namely the PIP_3 phosphatases phosphatase and tension homolog and Src homology 2 domain containing inositol 5′ phosphatase (17) or AKT (31). The relevance of these proteins in mediating phenotypes due to loss of dPIP4K function remains to be established. Whereas it is possible that phenotypes related to loss of dPIP4K function may be a consequence of elevated PI5P levels, changes in a quantitatively minor pool of $PI(4,5)P_2$ generated by PIP4K cannot be excluded. Further studies will be required to resolve these questions.

Materials and Methods

Fly Culture. Unless otherwise specified, flies (*Drosophila melanogaster*) were reared on standard medium containing agar, yeast, cornmeal, and dextrose, along with antibacterial and antifungal agents. Cultures were maintained at 23 °C and 50% relative humidity. The wild-type strain was Oregon-R.

Developmental Analysis of Growth. Flies were allowed to lay eggs for ≤4 h on cut bottles containing standard fly medium. Embryos were aged from the midpoint of that period. Newly hatched larvae were transferred to cut vials (20–25 larvae per vial) containing standard fly medium and reared at 23 °C until the required developmental stage. For each time point (4-h intervals during the day and 8-h interval at night) separate vials were set up and scored to count the number of larvae that had pupariated. For weight measurements, newly hatched larvae were transferred onto fresh medium and reared at 23 °C until the required developmental stage. Samples containing 10 larvae (n = 100 for each genotype) were measured using a precision balance (Sartorius; R160P).

Rapamycin Feeding. To measure the effect of rapamycin on development timing, groups of 20 newly hatched larvae from 4-h collection were placed in vials containing standard fly medium with or without 2 μM rapamycin (Sigma) and cultured at 23 °C until eclosion. Experiments were conducted in triplicate and the results were averaged.

Imaging and Analysis of Data. Complete experiments and appropriate control sets have been done by acquiring images on either an Olympus FV1000 laser scanning confocal microscope, using 20× objective (UPLAPO series, N.A. 0.7) or a Zeiss 510 LSM (with 405) Meta point-scanning confocal microscope, using a 20× (Plan Neofluar, N.A. 0.5) and processed using Fiji (ImageJ). The total volume of the gland and the number of nuclei measured using Volocity image analysis software were used to estimate the average cell size. A total of at least five salivary glands from a minimum of five animals were analyzed for each genotype. Statistical analysis of the data (two-tailed *T* test) was performed using Excel (Microsoft Office package).

Western Immunoblotting. Samples were separated using SDS/PAGE and electroblotted onto supported nitrocellulose membrane (Hybond-C Extra; GE Healthcare) using wet transfer assembly (Bio-Rad). Blots were incubated overnight at 4 °C in appropriate dilutions of primary antibody. Immunoreactive protein was visualized after incubation in 1:10,000 dilution of appropriate secondary antibody coupled to horseradish peroxidase (Jackson Immuno Research Laboratories) for 1 h at room temperature. Blots were developed with ECL (GE Healthcare) and imaged using a LAS 4000 instrument (GE Healthcare).

ACKNOWLEDGMENTS. P.R. acknowledges H. Okkenhaug for assistance with image analysis during an initial part of this work, A. Curwin for assistance with sucrose gradient experiments, and P. Georgiev for generating the UAS-dPIP4K:: GFP construct. This work was funded by the Biotechnology and Biological Sciences Research Council, United Kingdom, Department of Biotechnology, India, and the National Centre for Biological Sciences.

1. Church RB, Robertson FW (1966) Biochemical analysis of genetic differences in the growth of Drosophila. *Genet Res* 7(3):383–407.
2. Mirth CK, Riddiford LM (2007) Size assessment and growth control: How adult size is determined in insects. *Bioessays* 29(4):344–355.
3. Edgar BA (2006) How flies get their size: Genetics meets physiology. *Nat Rev Genet* 7(12):907–916.
4. Engelman JA, Luo J, Cantley LC (2006) The evolution of phosphatidylinositol 3-kinases as regulators of growth and metabolism. *Nat Rev Genet* 7(8):606–619.
5. Backer JM (2008) The regulation and function of Class III PI3Ks: Novel roles for Vps34. *Biochem J* 410(1):1–17.
6. Nobukuni T, et al. (2005) Amino acids mediate mTOR/raptor signaling through activation of class 3 phosphatidylinositol 3OH-kinase. *Proc Natl Acad Sci USA* 102(40): 14238–14243.
7. Hinchliffe KA, Ciruela A, Irvine RF (1998) PIPkins1, their substrates and their products: new functions for old enzymes. *Biochim Biophys Acta* 1436(1–2):87–104.
8. Rameh LE, Tolias KF, Duckworth BC, Cantley LC (1997) A new pathway for synthesis of phosphatidylinositol-4,5-bisphosphate. *Nature* 390(6656):192–196.
9. Zhang X, et al. (1997) Phosphatidylinositol-4-phosphate 5-kinase isozymes catalyze the synthesis of 3-phosphate-containing phosphatidylinositol signaling molecules. *J Biol Chem* 272(28):17756–17761.
10. van den Bout I, Divecha N (2009) PIP5K-driven PtdIns(4,5)P2 synthesis: Regulation and cellular functions. *J Cell Sci* 122(Pt 21):3837–3850.
11. Homma K, et al. (1998) Phosphatidylinositol-4-phosphate 5-kinase localized on the plasma membrane is essential for yeast cell morphogenesis. *J Biol Chem* 273(25): 15779–15786.
12. Kunz J, Fuelling A, Kolbe L, Anderson RA (2002) Stereo-specific substrate recognition by phosphatidylinositol phosphate kinases is swapped by changing a single amino acid residue. *J Biol Chem* 277(7):5611–5619.
13. Kunz J, et al. (2000) The activation loop of phosphatidylinositol phosphate kinases determines signaling specificity. *Mol Cell* 5(1):1–11.
14. Clarke JH, Wang M, Irvine RF (2010) Localization, regulation and function of type II phosphatidylinositol 5-phosphate 4-kinases. *Adv Enzyme Regul* 50(1):12–18.
15. Ciruela A, Hinchliffe KA, Divecha N, Irvine RF (2000) Nuclear targeting of the beta isoform of type II phosphatidylinositol phosphate kinase (phosphatidylinositol 5-phosphate 4-kinase) by its alpha-helix 7. *Biochem J* 346(Pt 3):587–591.
16. Jones DR, et al. (2006) Nuclear PtdIns5P as a transducer of stress signaling: An in vivo role for PIP4Kbeta. *Mol Cell* 23(5):685–695.
17. Carricaburu V, et al. (2003) The phosphatidylinositol (PI)-5-phosphate 4-kinase type II enzyme controls insulin signaling by regulating PI-3,4,5-trisphosphate degradation. *Proc Natl Acad Sci USA* 100(17):9867–9872.
18. Lamia KA, et al. (2004) Increased insulin sensitivity and reduced adiposity in phosphatidylinositol 5-phosphate 4-kinase beta$^{-/-}$ mice. *Mol Cell Biol* 24(11):5080–5087.
19. Clarke JH, Emson PC, Irvine RF (2008) Localization of phosphatidylinositol phosphate kinase IIgamma in kidney to a membrane trafficking compartment within specialized cells of the nephron. *Am J Physiol Renal Physiol* 295(5):F1422–F1430.
20. Rao VD, Misra S, Boronenkov IV, Anderson RA, Hurley JH (1998) Structure of type IIbeta phosphatidylinositol phosphate kinase: A protein kinase fold flattened for interfacial phosphorylation. *Cell* 94(6):829–839.
21. Morris JB, Hinchliffe KA, Ciruela A, Letcher AJ, Irvine RF (2000) Thrombin stimulation of platelets causes an increase in phosphatidylinositol 5-phosphate revealed by mass assay. *FEBS Lett* 475(1):57–60.
22. Montagne J, et al. (1999) Drosophila S6 kinase: A regulator of cell size. *Science* 285(5436):2126–2129.
23. Proud CG (2009) mTORC1 signalling and mRNA translation. *Biochem Soc Trans* 37(Pt 1):227–231.
24. Loewith R, et al. (2002) Two TOR complexes, only one of which is rapamycin sensitive, have distinct roles in cell growth control. *Mol Cell* 10(3):457–468.
25. Zhang H, Stallock JP, Ng JC, Reinhard C, Neufeld TP (2000) Regulation of cellular growth by the Drosophila target of rapamycin dTOR. *Genes Dev* 14(21):2712–2724.
26. Sarbassov DD, Guertin DA, Ali SM, Sabatini DM (2005) Phosphorylation and regulation of Akt/PKB by the rictor-mTOR complex. *Science* 307(5712):1098–1101.
27. Long X, Lin Y, Ortiz-Vega S, Yonezawa K, Avruch J (2005) Rheb binds and regulates the mTOR kinase. *Curr Biol* 15(8):702–713.
28. Ikeya T, Galic M, Belawat P, Nairz K, Hafen E (2002) Nutrient-dependent expression of insulin-like peptides from neuroendocrine cells in the CNS contributes to growth regulation in Drosophila. *Curr Biol* 12(15):1293–1300.
29. Sarkes D, Rameh LE (2010) A novel HPLC-based approach makes possible the spatial characterization of cellular PtdIns5P and other phosphoinositides. *Biochem J* 428(3): 375–384.
30. Gozani O, et al. (2003) The PHD finger of the chromatin-associated protein ING2 functions as a nuclear phosphoinositide receptor. *Cell* 114(1):99–111.
31. Ramel D, et al. (2009) PtdIns5P protects Akt from dephosphorylation through PP2A inhibition. *Biochem Biophys Res Commun* 387(1):127–131.